2021 43rd Annual International Conference of the
IEEE Engineering in Medicine & Biology Society (EMBC)
Oct 31 - Nov 4, 2021. Virtual Conference

Carbonized Polymer for Joule Heating Processing Towards Biosensor Development

Mohammad Aminul Haque[1], Nickolay V. Lavrik[2], Dale Hensley[2], Dayrl P. Briggs[2] and Nicole McFarlane[1]

***Abstract*— This paper presents the experimental findings towards developing carbonized microelectrodes using a Joule heating process within a temperature window that is compatible with CMOS. Bridge-on-pillars polymer structures have been 3D-printed using two-photon polymerization (2PP). They have been annealed in various processing conditions to increase the fraction of carbon in the precursor material and to achieve appreciable electric conductivity so that they can be used to drive current to enable Joule heating. To evaluate the outcome of the processing sequences, Raman spectroscopy has been performed to assess the degree of carbonization. Such CMOS-compatible carbon electrodes are important for monolithic, low-cost biosensor development.**

***Clinical relevance*— This establishes the potential of carbonized polymer electrode for low-cost, CMOS-compatible monolithic biosensor platform for implementation in medical diagnosis and treatment.**

I. Introduction

Integration of biocompatible electrodes and readout electronics has grabbed the attention of research in recent years [1]–[4]. Carbon-based materials are promising for biosensing electrode applications since they are chemically inert, show high electrical conductivity, and suitable for interfacing with biological systems in electrochemical sensors [5], [6]. Specifically, several studies of carbon nanotubes, graphene, and carbon nanofibers have shown promise in sensing, cell analysis, and human-robot interaction [7]–[12]. Integration of carbon-based electrodes with readout electronics is mostly implemented using separate platforms. This is due to the processing conditions required for carbon electrode fabrication which is not normally compatible with CMOS electronics. Recently, we have developed a processing sequence that enables carbonization of on-chip 3D printed microstructures suitable for biosensing applications. For 3D printing, we used a two-photon polymerization technique that can achieve resolution at sub-μm scale by exploiting femtosecond laser pulses for polymerization. Although our previous study demonstrated that a significant degree of carbonization can be successfully achieved within a CMOS compatible temperature window, more complete carbonization requires temperatures significantly above the CMOS compatible threshold of 700 °C [13]–[15].

[1]Mohammad Aminul Haque and Nicole McFarlane are with Electrical Engineering and Computer Science, The University of Tennessee, Knoxville, Tennessee, 37996, USA. mhaque4@vols.utk.edu

[2]Nickolay V. Lavrik, Dayrl P. Briggs and Dale Hensley are with Center for Nanophase Materials Sciences, Oak Ridge National Laboratory, Oak Ridge, Tennessee, 37830, USA. lavriknv@ornl.gov

To address this issue, we plan to exploit localized heating induced by electric currents, commonly termed as Joule heating. To explain this idea further, we would like to drive current through the partially pyrolyzed polymer so that it heats up locally and self-pyrolyzes even more completely thereby transforming into a pure carbon material through this process. While localized Joule heating method was shown to be very promising for a variety of emerging applications, to the best of our knowledge, it has not been applied to carbonization of 3D printed polymer structures. As a preliminary step of implementing this novel concept, we focus on establishing experimental conditions for producing mechanically and structurally stable partially pyrolyzed structures that would be suitable for additional localized Joule heating anneal due to an external voltage.

Despite its clear potential, this approach involves several technological and design challenges. First of all, in order to conduct current, electrically insulating polymer structures need to be converted into a carbon-rich material with appreciable electric conductivity. This step needs to remain within the CMOS-compatibile technological window. To address this challenge, instead of simple cone or pillars structures explored in our previous studies [13]–[15], the present study focuses on newly designed structures that facilitate biasing across the device for the proposed localized Joule heating. In our previous studies, we observed that 3D printed polymer structures tend to shrink and deform significantly during the pyrolysis. Thus, one of the main goals of the present study is to verify that the structures printed according to these new designs can withstand initial thermal processing physically and mechanically. And finally more specifically, in this preliminary study we seek to verify that the 3D printed and subsequently partially pyrolyzed structures can form stable connections with metal electrodes to enable biasing.

II. Experiment

The experimental steps of the present study stem from our previous work on CMOS-compatible microelectrode fabrication [13]–[15]. However, addressing distinct technological challenges as mentioned above requires modification of several processing steps. We use a platinum-on-titanium metal stack as the electrode. Titanium provides adhesion and platinum provides better thermal stability. Specifically, 10 nm titanium (Ti) and 50 nm platinum (Pt) metal stacks were used as electrodes. The electrode layouts were generated in the industry standard GDSII format for photolithographic mask fabrication. The

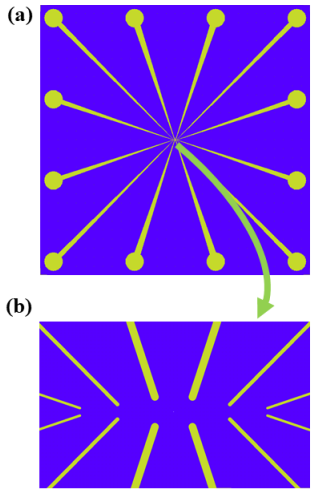

Fig. 1. Layout of a chip with 6 pairs of photolithographically patterned metal electrodes. (a) Layout of the entire chip. (b) Zoomed-in center section where 6 bridge-on-pillars structures were 3D-printed using 2PP.

TABLE I
DIMENSIONS OF DESIGNED POLYMER BRIDGE-ON-PILLARS STRUCTURES 3D-PRINTED USING 2PP.

Structure	Pillar		Bridge	
	Height (μm)	Diameter (μm)	Length (μm)	Diameter (μm)
S	5	10	5	2
M	10	10	10	2
L	20	10	20	2

electrodes were patterned on a 100 mm silica wafer using a sequence of contact photolithography and metal lift off. The wafer was then diced into 15 mm × 15 mm chips using an Accretech dicing saw (Accretech-SS10). The layout of the patterned single chip is shown in Fig. 1, where Fig. 1 (a) shows the layout of a single chip, and Fig. 1 (b) shows the zoomed-in view of the center where the bridge-on-pillars structures were to be printed. The distances between the electrodes were selected to match the bridge lengths of 5, 10, and 20 μm in the bridge-on-pillar structures that are subsequently printed using the 2-photon polymerization (2PP) technique.

Bridge-on-pillars structures were 3D printed using the commercially available 2PP tool (Nanoscribe Photonic Professional GT). Using the Nanoscribe supplied photopolymer, IP-S, we printed three different sizes of structures with the dimensions listed in Table I. It needs to be noted that high laser power can cause cavitation (bubble formation) on the metallized silica substrate. This can lead to defects on the printed structures even if the laser power is otherwise optimized for the 2PP printing. Once the structures were written, uncrosslinked IP-S was washed away by immersing the samples in SU-8 developer for 20 minutes followed by bathing in isopropanol and blow drying with filtered nitrogen.

Similar to standard carbon fiber manufacturing protocols and our previous work on polymer carbonization [13]–[15], we used a two-step annealing process for polymer carbonization. The first step involved a stabilizing anneal on a heated stage (Linkam Scientific LTS420E-P) in the ambient atmosphere. In this step, we heated the chip and held it at 340 °C for 10 minutes in the presence of air to initialize oxidation. The next step involved a carbonizing anneal in argon (Ar) at 500-600 °C for 10-30 minutes in a rapid thermal processing tool (First Nano EasyTube® 3000). To characterize the structures, a scanning electron microscope (Zeiss Merlin) was used to image the structures before and after the different processing steps. The degree of carbonization was determined using Raman spectroscopy (Renishaw InVia).

III. Results and Discussion

SEM images of as-printed bridge-on-pillars structures are shown in Fig. 2 (a)-(b), where Fig. 2 (a) shows an array of structures with the dimensions given in Table I, and Fig. 2 (b) shows a single bridge-on-pillars structure with geometrical dimensions of the structure 'S' as specified in Table I. There are some defects on the structures. These defects were due to occasional cavitation during the printing process as explained above. It can also be seen that there are some defects on the metal electrodes, which can be reduced by refining the combination of metal evaporation and photolithographic patterning steps.

In order to have a good electrical conductance through the bridge-on-pillars structure, it needs to have a high carbon content. Thus structures were heated on a hot plate and held at 340 °C for an oxidative anneal followed by increased anneal time up of to 60 minutes (split into two 30 minutes periods) at 500 °C. In a separate consecutive processing sequence, structures were heated on a hot plate and held at 340 °C for an oxidative anneal which was followed by an inert atmosphere (Ar) anneal at 500 °C (for 10 and 30 minutes, respectively) and 600 °C (for 10 and 30 minutes, respectively). Conditions of these processing steps are given in Table II.

Structures were then observed using SEM to verify their structural robustness after multiple annealing steps. Fig. 2 (c) shows SEM image of a larger structure (Structure L_{560} in Table II) after an oxidative anneal at 340 °C and an inert atmosphere anneal at 500 °C for 60 minutes, and Fig. 2 (d) shows SEM image of the smaller structure (S_{560} of Table II) processed through similar steps.

From Fig. 2, the structures have been found to be physically stable and maintain good connection with the metal electrodes after printing and after oxidative and inert atmosphere anneals. Subsequent annealing steps confirmed that they can also withstand repeated high temperature annealing. One clear observation from Fig. 2 (c)-(d) is that smaller structures with shorter bridge elements are more severely affected by the high degree of volumetric shrinkage compared to the larger ones due to their higher susceptibility to tensile stresses. A significant amount of shrinkage was observed in all cases which is consistent with our previous

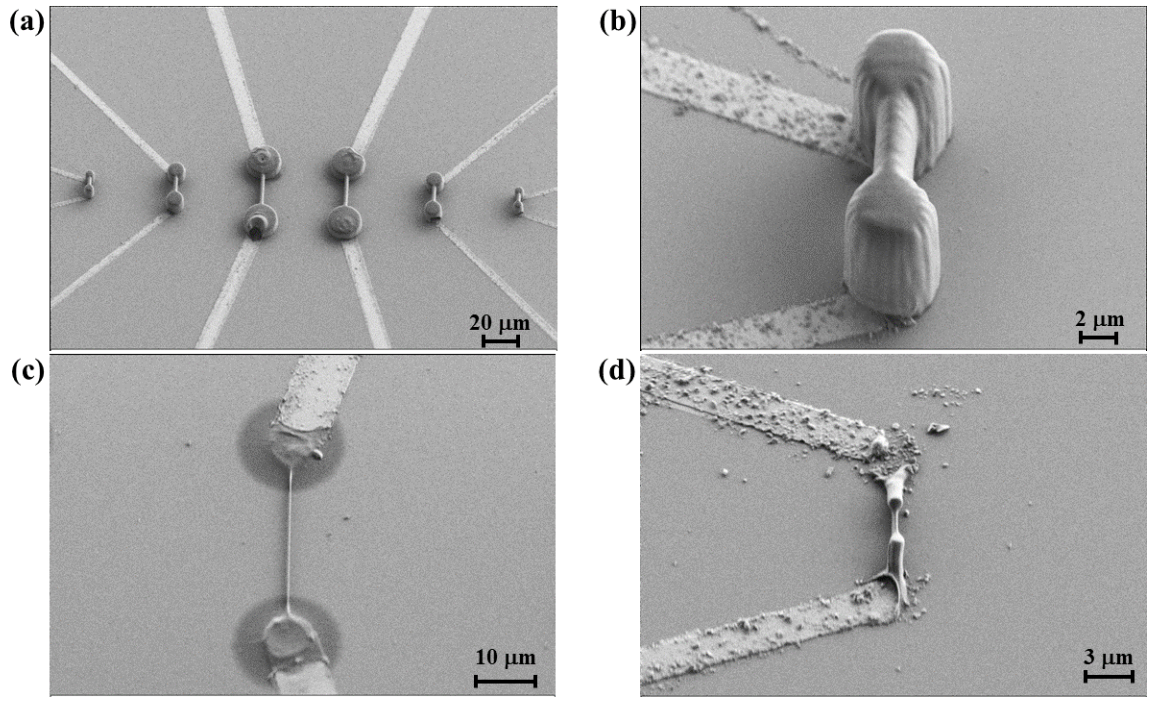

Fig. 2. Bridge-on-pillars structures before and after high temperature processing sequence. (a) An array of as-printed pridge-on-pillar polymer structures with the dimensions listed in Table 1. (b) As-printed polymer structure corresponding to sample S listed in Table 1. (c)-(d) Bridge-on-pillar structures (labelled L and S, respectively, in Table 1) processed through an oxidative anneal at 340 ^{0}C for 10 minutes on hot plate followed by an inert atmosphere anneal at 500 ^{0}C for 60 minutes in RTP.

TABLE II

VARIOUS SEQUENCES OF OXIDATIVE AND INERT ATMOSPHERE ANNEAL PROCESSING STEPS EXPLORED IN THE PRESENT STUDY AND CORRESPONDING LABELLING OF THE SAMPLES.

Consecutive processing steps	**S**	**M**	**L**
1. Oxidative anneal at 340 °C on hot plate and holding for 10 mins	S_{310}	M_{310}	L_{310}
Multiple Consecutive Anneals			
2. (a)-1: Anneal in Ar at 500 °C for 10 minutes	S_{510}	M_{510}	L_{510}
2. (a)-2: Anneal in Ar at 500 °C for 30 minutes	S_{530}	M_{530}	L_{530}
2. (a)-3: Anneal in Ar at 600 °C for 10 minutes	S_{610}	M_{610}	L_{610}
2. (a)-4: Anneal in Ar at 600 °C for 30 minutes	S_{630}	M_{630}	L_{630}
Single Anneal			
2. (b): Anneal in Ar at 500 °C for 60 minutes	S_{560}	M_{560}	L_{560}

observations [13]. The inward deformation of pillars during annealing can be attributed to the mechanical tensile stresses exerted on the pillars due to shrinkage of the bridge. Designs that are less prone to such deformations can be based on spiral bridge elements that would minimize tensile stresses exerted on pillars during anneal.

Our previous work showed that the oxidative anneal followed by a single anneal in an inert atmosphere at 500 °C for 10 minutes leads to the formation of a partially pyrolyzed precursor characterized by a strong background fluorescence in Raman spectroscopy. Therefore, a higher temperature anneal is likely required to obtain a higher degree of carbonization. However, CMOS compatibility restricts the use of temperatures beyond 550 °C. Raman spectroscopy of samples L_{560} and S_{560} processed at various other conditions specified in Table II was conducted to evaluate their degree of carbonization. As expected, increased annealing time reduces background fluorescence and, therefore, increases the degree of carbonization. Samples M_{510}-M_{560} showed similar behavior. Fig. 3 and Fig. 4 show the Raman spectra taken on the bridge sections and pillar sections, respectively. The two recognizable peaks at 1346 cm^{-1} and 1586 cm^{-1} correspond to the D and G bands. The D-band is also known as the defect band. It is caused by graphene-associated vibrational modes. G-band is associated with sp^2 bonded carbon in planar sheets. Fig. 4 generates smoother and higher signal-to-noise ratios in the Raman spectra compared to Fig. 3, which are likely due to the presence of a larger quantity of material in the pillar sections compared to the bridge section.

IV. CONCLUSION

In this work, we have designed, 3D printed and partially carbonized bridge-on-pillars structures on silica substrates with photolithographically patterned metal electrodes. Partial carbonization of the 3D printed structures was achieved within a CMOS-compatible temperature window. According to the Raman spectroscopy data obtained, progressively higher degrees of carbonization could be achieved not only

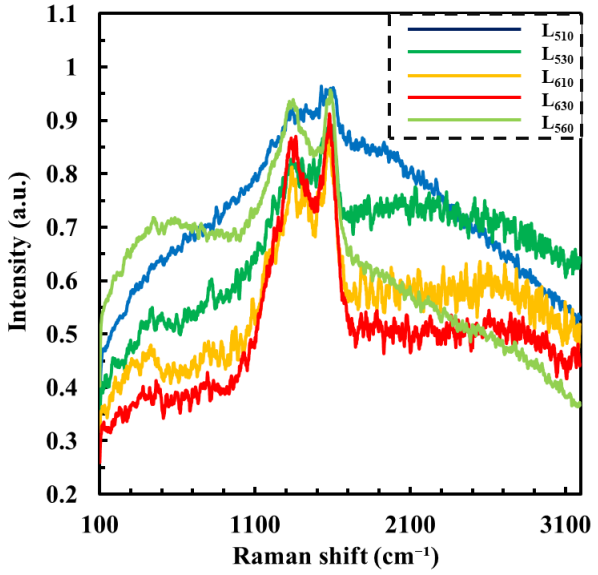

Fig. 3. Raman spectroscopy of bridge sections of samples L_{510}-L_{560} processed at different processing conditions of Table II.

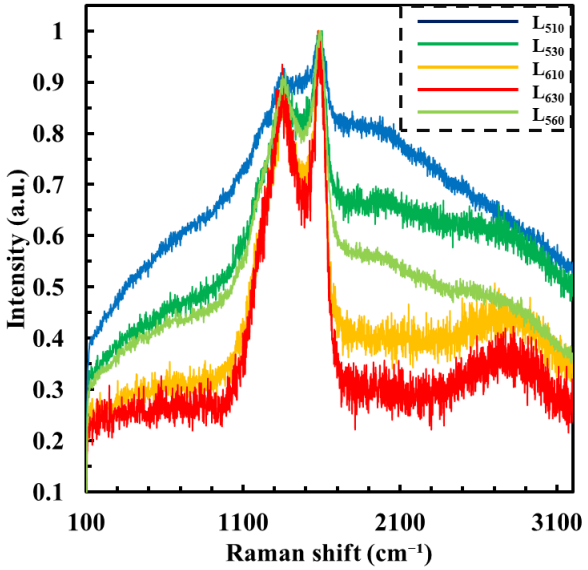

Fig. 4. Raman spectroscopy of pillar sections of samples L_{510}-L_{560} processed at different processing conditions as specified in Table II.

by annealing at a higher temperature but also by increasing the annealing time. These preliminary experimental findings indicate that even higher degrees of carbonization may be possible by conducting pyrolysis at 500 °C for more than 1 hour. Thus, this approach has the potential to provide sufficiently high electric conductivity necessary to implement localized Joule heating to achieve complete carbonization. The fabrication and processing of 3D printed structures demonstrated in the present work addresses several technological challenges, such as mechanical stress, shrinkage, and structural stability. However, our preliminary results show that the structures adhere well to the metal electrodes and they can withstand high temperature processing. These findings pave the way towards developing a cost-efficient, monilithic biosensor platform.

Acknowledgement

Design, fabrication and characterization of the samples involved in this research was conducted at the Center for Nanophase Materials Sciences, which is a DOE Office of Science User Facility.

References

[1] Y. Jia, B. Lee, F. Kong, Z. Zeng, M. Connolly, B. Mahmoudi, and M. Ghovanloo, "A software-defined radio receiver for wireless recording from freely behaving animals," *IEEE Transactions on Biomedical Circuits and Systems*, vol. 13, no. 6, pp. 1645–1654, 2019.

[2] W. T. Navaraj, H. Nassar, and R. Dahiya, "Prosthetic hand with biomimetic tactile sensing and force feedback," in *IEEE International Symposium on Circuits and Systems*, Sapporo, Japan, May 2019, pp. 1–4.

[3] M. A. Hari and L. Rajan, "Advanced materials and technologies for touch sensing in prosthetic limbs," *IEEE Transactions on NanoBioscience*, 2021.

[4] G. Panuccio, M. Semprini, L. Natale, S. Buccelli, I. Colombi, and M. Chiappalone, "Progress in neuroengineering for brain repair: New challenges and open issues," *Brain and neuroscience advances*, vol. 2, p. 2398212818776475, 2018.

[5] A. S. Shanta, K. A. Al Mamun, D. Hensley, N. V. Lavrik, S. K. Islam, and N. McFarlane, "Carbon nanospikes for biosensing applications," in *Annual International Conference of the IEEE Engineering in Medicine and Biology Society*, Jeju, Korea (South), July 2017, pp. 193–196.

[6] A. S. Shanta, S. Shamsir, Y. Song, D. K. Hensley, A. J. Rondinone, S. K. Islam, and N. McFarlane, "Carbon nanospikes on silicon wafer for amperometric biosensing applications," in *Annual International Conference of the IEEE Engineering in Medicine and Biology Society*, Honolulu, HI, July 2018, pp. 4281–4284.

[7] J. D. Harvey, H. A. Baker, M. V. Ortiz, A. Kentsis, and D. A. Heller, "HIV detection via a carbon nanotube RNA sensor," *ACS sensors*, vol. 4, no. 5, pp. 1236–1244, 2019.

[8] J. A. Stapleton, E. M. Hofferber, J. Meier, I. A. Ramirez, and N. M. Iverson, "Single-walled carbon nanotube sensor platform for the study of extracellular analytes," *ACS Applied Nano Materials*, vol. 4, no. 1, pp. 33–42, 2020.

[9] S. K. Ameri, M. Kim, I. A. Kuang, W. K. Perera, M. Alshiekh, H. Jeong, U. Topcu, D. Akinwande, and N. Lu, "Imperceptible electrooculography graphene sensor system for human–robot interface," *NPJ 2D Materials and Applications*, vol. 2, no. 1, pp. 1–7, 2018.

[10] Y. Kim, T. Kim, J. Lee, Y. S. Choi, J. Moon, S. Y. Park, T. H. Lee, H. K. Park, S. A. Lee, M. S. Kwon *et al.*, "Tailored graphene micropatterns by wafer-scale direct transfer for flexible chemical sensor platform," *Advanced Materials*, vol. 33, no. 2, p. 2004827, 2021.

[11] Z. Wang, S. Wu, J. Wang, A. Yu, and G. Wei, "Carbon nanofiber-based functional nanomaterials for sensor applications," *Nanomaterials*, vol. 9, no. 7, p. 1045, 2019.

[12] S. A. Chowdhury, M. C. Saha, S. Patterson, T. Robison, and Y. Liu, "Highly conductive polydimethylsiloxane/carbon nanofiber composites for flexible sensor applications," *Advanced Materials Technologies*, vol. 4, no. 1, p. 1800398, 2019.

[13] M. A. Haque, N. V. Lavrik, A. Hedayatipour, D. Hensley, D. P. Briggs, and N. McFarlane, "Carbonization of 3D printed polymer structures for CMOS-compatible electrochemical sensors," *Journal of Vacuum Science & Technology B, Nanotechnology and Microelectronics: Materials, Processing, Measurement, and Phenomena*, vol. 38, no. 5, p. 052203, 2020.

[14] M. A. Haque, N. McFarlane, N. V. Lavrik, and D. Hensley, "Carbonized polymer nanostructures for biosensing," in *Annual SEMI Advanced Semiconductor Manufacturing Conference*, Saratoga Springs, NY, May 2019, pp. 1–5.

[15] M. A. Haque, N. V. Lavrik, D. Hensley, and N. McFarlane, "Carbonized electrodes for electrochemical sensing," in *IEEE Electronic Components and Technology Conference*, Las Vegas, NV, May 2019, pp. 2073–2078.